Journal of Nuclear Materials 386–388 (2009) 395–399

Contents lists available at ScienceDirect

Journal of Nuclear Materials

journal homepage: www.elsevier.com/locate/jnucmat

Post-implantation thermal desorption of helium from poly- and single-crystalline iron

Donghua Xu *, Brian D. Wirth [1]

Department of Nuclear Engineering, University of California, Berkeley, CA 94720-1730, USA

A B S T R A C T

Helium desorption is studied on both poly- (PC) and single-crystalline (SC) iron during constant rate heating following room temperature He ion implantations. A sharp desorption peak due to the BCC–FCC phase transformation is observed for both PC and SC specimens under all examined implantation conditions, which provides precise temperature calibration. Within the BCC structural range, three groups (I: below 300 °C; II: 300–600 °C; III: 600–900 °C) of desorption signal are identified for PC specimens while only two groups (I: below 300 °C; II: 550–900 °C) are identified for SC specimens. The low T group generally appears broader in PC specimens. PC and SC desorption spectra show similar dependence on implantation energy and fluence, namely that the relative intensity at low and intermediate temperatures decreases with increasing implantation energy or fluence, while the fluence effect is much more pronounced than the energy effect. Simple first order dissociation kinetics are used to estimate the average activation energies associated with the desorption groups. The present data for SC iron are expected to provide an appropriate experimental reference for future rate-theory or kinetic Monte–Carlo modeling of helium defect evolution in BCC iron.

1. Introduction

Helium effects on the microstructure and mechanical properties are among the most important subjects in fusion materials research. It has been shown that the high level of implanted or transmutationally produced (by high energy neutron flux) helium under fusion conditions can cause nucleation and growth of helium bubbles in structural materials and subsequently result in significant mechanical property degradation [1–4]. The key to understanding helium effects is to determine the mechanisms by which helium atoms migrate and interact with various microstructural features in irradiated materials. This is an inherently multi-scale problem spanning from atomistic to macro-scopic dimensions in both time and space.

At the atomistic level, computer simulations using ab initio and Molecular Statics/Dynamics approaches have been performed to investigate the kinetics, energetics and thermal stabilities of He and small He-containing clusters, and the He interactions with dislocations and grain boundaries in BCC iron [5–12]. On the nano-, micro- or macro-scopic level, experiments using optical or electron microscopy, nuclear reaction depth profiling, positron annihilation spectroscopy, coincidence Doppler broadening, thermal desorption and other techniques have been conducted to analyze He behavior and the coupled He and defect evolution in BCC iron and ferritic alloys [13–18]. More recently, continuum rate-theory modeling [19] has been compared to isothermal He desorption from BCC iron to validate ab initio results.

All previous thermal helium desorption experiments on iron appear to have only used poly-crystalline (PC) specimens. It is thus not clear whether the grain boundary has made any contribution to the resulting desorption signals. For the purpose of validating fundamental parameters such as migration or binding energies of He and He-V clusters, single-crystalline specimens are more appropriate. In this paper we report results from thermal desorption experiments on high purity specimens, which consisted of both poly-crystalline and single crystal (SC) iron, following room temperature ^{4}He ion implantations at selected energies and fluences. Similarities and distinctions between the Helium desorption spectra for the PC and SC specimens, along with their dependence on implantation energy and fluence will be presented here. The desorption spectra have been analyzed using simple first order dissociation kinetics to obtain an estimate for the activation energies associated with the observed desorption signals.

2. Experimental

High purity (99.95%) PC iron plates were purchased from Alfa Aesar. High purity (99.94%) SC iron disks were provided by Dr

* Corresponding author. Tel.: +1 510 643 3281.
E-mail addresses: xudh@nuc.berkeley.edu (D. Xu), bdwirth@nuc.berkeley.edu (B.D. Wirth).
[1] Tel.: +1 510 642 5341.

0022-3115/$ - see front matter © 2009 Elsevier B.V. All rights reserved.
doi:10.1016/j.jnucmat.2008.12.141

S.A. Maloy at Los Alamos National Laboratory. Small specimens ($\sim$0.5–1 × 2.5 × 3.5 mm) were cut from the plates or disks, mechanically polished to 1 μm grade smoothness, and then commercially implanted at room temperature with ^{4}He ions at 5 or 10 keV to fluences of 10^{14} or 10^{15} He/cm^2. The implantation flux was $\sim$7–10 × 10^{10} He/cm^{2}s. Grain size of the PC specimens was determined to be on the order of 50 μm through optical microscopy observations.

Partial He current was measured in our ultrahigh vacuum thermal desorption system (TDS) [20] as a function of temperature during constant rate (1 K/s) thermal ramping on each of these He-implanted specimens from room temperature up to 1300 °C. The He current was then converted to the instantaneous desorption rate by multiplying a proportionality coefficient, determined separately with a calibration procedure. More details regarding our TDS system are available in Ref. [20].

3. Results and discussion

3.1. Trim/SRIM calculations

Probabilistic depth distributions of generated Frenkel pairs and stopped ^{4}He ions during implantation in iron were evaluated using SRIM 2003 software [21]. For 5 and 10 keV implantation energies, the maximum production of Frenkel pairs occurs at $\sim$12 and 26 nm below the implantation surface, while the maximum in the distribution of He occurs at 25 and 50 nm, respectively. On the average, 20 and 33 Frenkel pairs are generated per He ion for the two energies, respectively. These values correspond to a peak displacement damage of $\sim$85 and 75 mdpa, and a peak He concentration of 2830 and 1760 appm for the two energies, respectively, at a fluence of 10^{15} He/cm^2.

3.2. Background signal

In an earlier publication [20], we noted the possibility of spurious background signals interfering with real desorption spectra and causing problems in data analysis. It is thus very critical to have a clean background in order to obtain reliable desorption data. By enhancing the cooling of the chamber walls, the problem of spurious background signals in our system has been solved. The background He current from non-implanted control specimens now remains almost constant at a low value of $\sim 6 \times 10^{-13}$ A from room temperature up to 1300 °C. In addition, the total pressure of our system is now also very low ($\sim 1 \times 10^{-9}$ Torr) and stable over the entire temperature range.

3.3. General features of PC spectra and effects of implantation energy and fluence

The He desorption spectra obtained from PC specimens for the four combinations of implantation energies and fluences used in this work are presented in Fig. 1(a)–(d). Two general features of the desorption spectra can be noticed from Fig. 1. First, there exists a sharp peak for each of the spectra, which due to its excessive sharpness is not consistent with a first order dissociation model as generally adopted in classical rate-theory. Such a sharp peak has also been observed for PC iron and ferritic alloys under other implantation conditions [17,20]. In Ref. [20], we discussed the strong evidence leading to the conclusion that this peak is primarily due to the alpha–gamma (BCC–FCC) phase transformation [22]. Therefore, in this work, we have used this peak to calibrate our thermocouple temperature readings by setting the peak position to 912 °C (the well known value of the alpha–gamma transformation in pure iron) and using a linear-correction to the other temperature values. It should be pointed out that the exact mechanism of the sharp He release peak at the alpha–gamma phase transformation remains unclear. Sugano et al. [17] interpreted this sharp peak as evidence for the lower stability of He-vacancy clusters in FCC iron than in BCC iron. This argument, nevertheless, can not explain the re-appearance of the peak during cooling as reported in Ref. [20], since in that case the specimen transforms back from the FCC to BCC structure. Ono et al. [14] have considered this sharp release peak as a result of transient structural instability (by shearing or sweeping of phase boundaries for example) around helium micro-bubbles during the phase transformation. This interpretation appears more reasonable since the structural instability can occur both upon heating and cooling as long as the phase transformation takes place.

The second general feature of the observed He desorption in PC specimens is that the release signal can be divided into three groups within the BCC structural range (prior to the alpha–gamma phase transformation), as shown in Fig. 1(a)–(d). Group I lies on the low T side, spanning from room temperature up to around 300 °C, Group II in the intermediate T range, from 300 °C to 600 °C, and Group III in the high T range, from 600 °C to $\sim$900 °C ending with the sharp peak induced by the alpha–gamma phase transformation. Above 912 °C, i.e., in the FCC structural range, there is another group of release signal which will be called FCC Group in the subsequent context. Here the word 'Group' is used instead of 'Peak' because each 'group' requires more than one single (defined by a definite activation energy) dissociation event to reasonably reproduce the peak width and thus, may involve multiple dissociation mechanisms [23].

By comparing the four desorption spectra from the PC specimens, the effects of varying implantation energy and fluence can be recognized. For example, at a fixed energy of 5 keV, as the He fluence increases from 10^{14} (Fig. 1(a)) to 10^{15} (Fig. 1(b)) He/cm^2, the relative strengths (intensities) of Group I and Group II at low and intermediate T with respect to the entire spectrum apparently decrease while that of the high T release in the FCC phase apparently increases. Similar trends can be noticed when spectra corresponding to a common He fluence, but with increasing implantation energies are compared. However, it is evident from Fig. 1(a)–(d) that the effect of varying He fluence is much more significant than that of varying He energy, at least within the range of fluence and energy in the present study.

3.4. General features of SC spectra – similarities and distinctions with respect to PC spectra

As shown in Fig. 2(a)–(d), the He desorption spectra from the SC specimens display certain similarities and distinctions when compared with the PC spectra shown in Fig. 1(a)–(d). Similar to the PC spectra, the SC spectra also exhibit the sharp alpha–gamma phase transformation peak, and again this peak has been used to calibrate the temperature readings. The second similarity involves the existence of multiple He release groups in well-separated temperature ranges, although there are differences in the details of each grouping. Third, the SC spectra exhibit similar effects of implantation energy and fluence as the PC spectra.

The SC spectra are distinct from the PC spectra in the following three aspects. First, the SC spectra only comprise two groups of signal within the BCC structural range, Group I from room temperature to 300 °C, and Group II from about 550 °C to 900 °C, with no obvious signal between 300 °C and 550–600 °C as in the PC spectra (Group II, PC). Second, Group I (except the 5 keV and 10^{15} He/cm^2 case) at low T, as well as the release within the FCC phase at very high T (in all cases), are both narrower in SC than in PC. Third, the major desorption group (Group III for PC, Group II for SC) appears to have more splittings, or fine-scale structure in the SC specimens

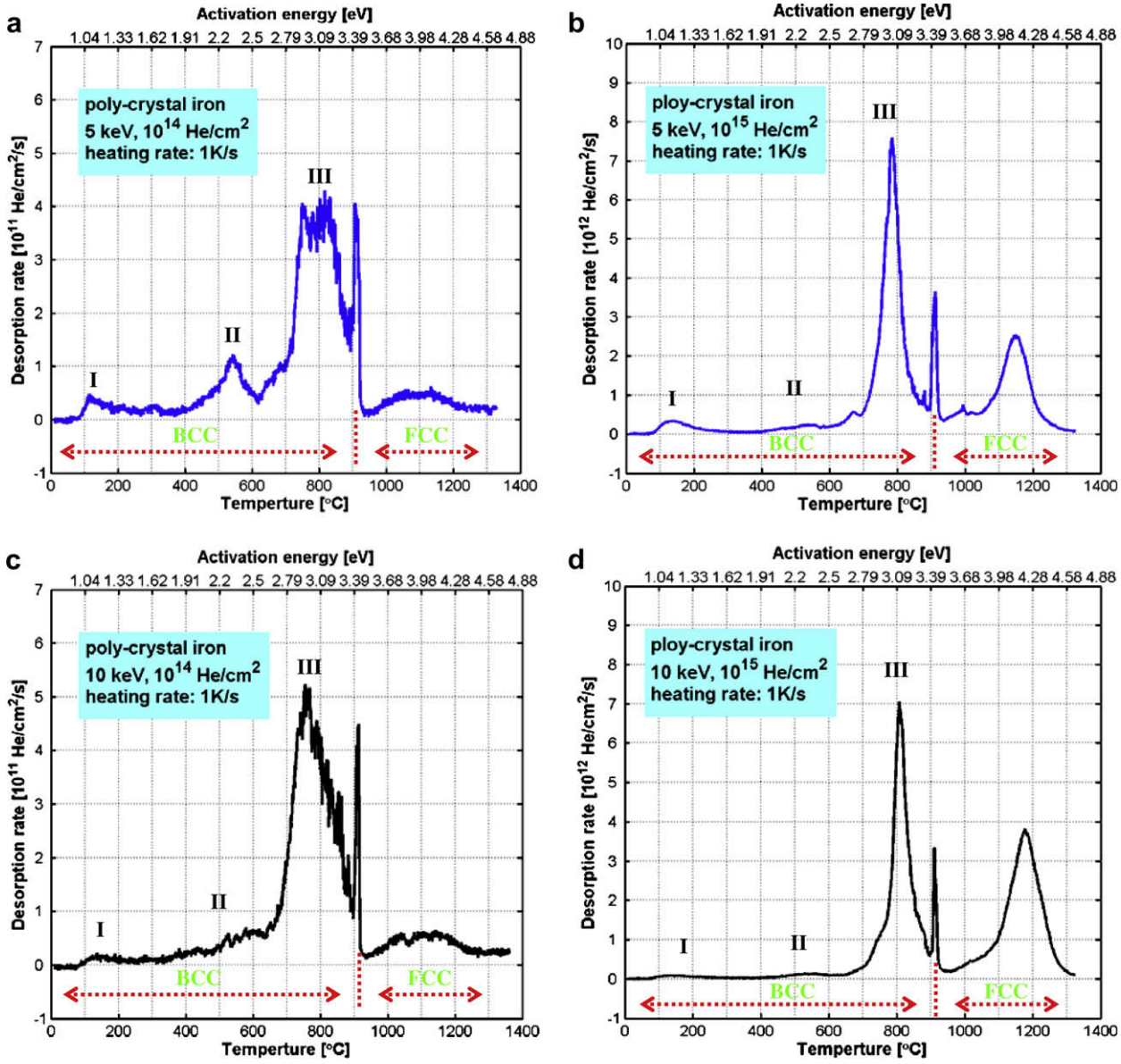

Fig. 1. Desorption spectra of high purity polycrystalline iron implanted with ^{4}He at: (a) 5 keV, 10^{14} He/cm^2; (b) 5 keV, 10^{15} He/cm^2; (c) 10 keV, 10^{14} He/cm^2; (d) 10 keV, 10^{15} He/cm^2.

than in the PC. The above three aspects, when viewed together, are actually consistent in that they reflect a common distinction between SC and PC spectra: SC spectra are less diffuse than PC spectra.

It is tempting to ascribe the less diffuse character of SC spectra to the absence of grain boundaries, considering the wide range of He trapping strength (binding energies) that can be provided by grain boundaries of different structures, particularly associated with excess volume in the boundaries [12]. One may notice that the total TRIM/SRIM He penetration depth is below or slightly above 100 nm at the present implantation energies which is much smaller than the average PC grain size (~50 μm). Nevertheless, the grains and their boundaries in the PC specimens are randomly distributed both along the depth and transverse directions (implantation beam perpendicular to the surface). Further, as consistently indicated by all the atomistic calculations [5–7], the migration of a He interstitial prior to its capture by various traps is extremely fast with an energy barrier as low as 0.06 or 0.08 eV which corresponds to a diffusion length of several to several tens of microns (depending on the diffusivity prefactor) within one second at room temperature. The positive binding energies of He with grain boundaries can thus effectively drive additional diffusion towards the boundaries resulting in the trapping of He to the boundaries and hence the spreading of overall He trapping strength. Besides grain boundaries, impurities and dislocation densities may also play important roles in He-participated defect evolution. However, in the present study, the purities of PC (99.95%) and SC (99.94%) specimens are very close and both very high, and the dislocation densities, although not measured, are expected to be on the same level for PC and SC based on the processing procedure. As such, compared with grain boundaries, these two latter factors are presumed to make only insignificant contributions to the distinctions observed between PC and SC specimens.

Additional investigations involving more systematic modifications of grain size would be a useful extension of the present work to further confirm the effects of grain boundaries. To provide interpretation of the detailed release mechanisms, we are currently in the process of developing a spatially-dependent cluster dynamics

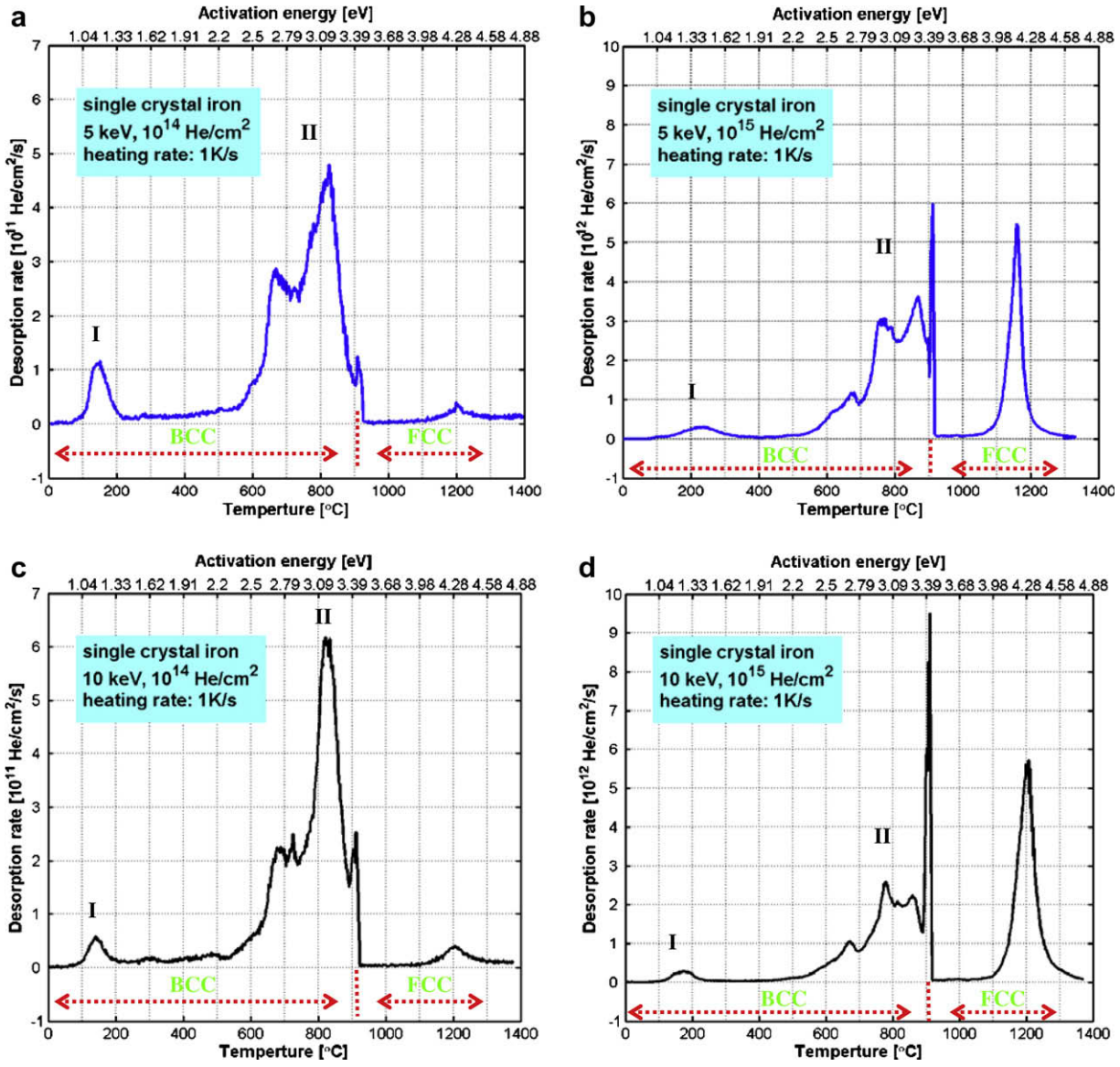

Fig. 2. Desorption spectra of high purity single-crystalline iron implanted with ^{4}He at: (a) 5 keV, 10^{14} He/cm^2; (b) 5 keV, 10^{15} He/cm^2; (c) 10 keV, 10^{14} He/cm^2; (d) 10 keV, 10^{15} He/cm^2.

model which tracks the temporal evolution of He, V and I clusters in both phase space and real space. Yet, the present results evidently show that the desorption behavior of iron is indeed influenced by the presence or absence of grain boundaries and therefore, caution should be taken when comparing rate-theory or kinetic Monte–Carlo modeling results with experimental data collected from PC specimens. As a matter of fact, the present SC spectra are expected to provide additional, and perhaps more appropriate experimental reference for future modeling work.

3.5. Activation energies

In both Figs. 1 and 2, we have included an energy scale as the top axis, in correlation with the bottom temperature scale. The displayed energy values were calculated based on simple first order dissociation kinetics, i.e., $\frac{d}{dt}N = -Nf\exp(-\frac{E}{k_BT})$, where N is the remaining number of He atoms not yet desorbed from a specific trap, f is the jumping frequency (assumed to be 10^{13}/s), E is the activation energy for the trap, and k_BT has its normal meaning. Within this model, it is straightforward to derive the relationship among peak temperature T_p, heating rate R, and activation energy E, i.e., $\ln(R/T_p^2) = -E/k_BT_p + \ln(fk_B/E)$ [20], which provides a one to one correlation between peak temperature and activation energy at chosen R (here 1 K/s) and f values. It should be noted that this simple model has assumed that there are no mutual transformations among traps with different E values, which is certainly not the real case since evolution among different traps/defect-clusters with distinct E values is unavoidable. However, this simple model can provide an estimate for the average E values of a group of traps which have mutual transformation among themselves and yet sufficiently separated from other groups with respect to E values.

4. Summary

We have performed helium desorption experiments on both poly- (PC) and single (SC) crystalline iron under nearly identical conditions. Our results reveal both similarities and distinctions between the two types of specimens. The similarities include the appearance of a sharp release peak induced by the alpha–gamma phase transformation, the existence of multiple desorption groups,

and the influence of varying implantation energy and fluence on the desorption behavior. The essential distinction is that SC spectra are less diffuse than PC spectra, which is reflected in three details: (i) within the BCC structural range, SC spectra comprise only two groups of signal as opposed to three observed in PC spectra; (ii). Group I generally appears narrower for SC than for PC; (iii). Group II of SC displays more fine-scale structure than Group III of PC despite their similar temperature range. Average activation energies associated with the observed desorption groups have been estimated based on simple first order dissociation kinetics. While the underlying microscopic mechanisms for all the desorption groups are not entirely clear at this stage, our result suggests that it may not be advisable to compare rate-theory or kinetic Monte–Carlo modeling which does not include grain boundaries with desorption experiments conducted on PC specimens. The present desorption data from SC iron are expected to provide an additional, and perhaps more appropriate experimental reference for future modeling.

Acknowledgements

The authors thank Dr Stuart A. Maloy (LANL) for providing the single crystal Fe specimens, and Drs. Maria Jose Caturla (University of Alicante), Chu-Chun Fu (CEA-Saclay), Christophe Ortiz (University of Alicante), and Kazunori Morishita (University of Kyoto) for helpful discussions. This work has been supported by the Office of Fusion Energy Sciences, US Department of Energy, under Grant DE-FG02-04ER54750.

References

[1] L.K. Mansur, W.A. Coghlan, J. Nucl. Mater. 119 (1983) 1.
[2] H. Ullmaier, Nucl. Fusion 24 (1984) 1039.
[3] L.K. Mansur, M.L. Grossbeck, J. Nucl. Mater. 155 (1988) 130.
[4] H. Trinkaus, B.N. Singh, J. Nucl. Mater. 323 (2003) 229.
[5] K. Morishita, R. Sugano, B.D. Wirth, T.D. de la Rubia, Nucl. Instrum. and Meth. Phys. Res. B 202 (2003) 76.
[6] B.D. Wirth et al., J. Nucl. Mater. 329 (2004) 103.
[7] C.C. Fu, F. Willaime, Phys. Rev. B 72 (2005) 064117.
[8] L. Ventelon, B.D. Wirth, C. Domain, J. Nucl. Mater. 351 (2006) 119.
[9] T. Seletskaia, Y.N. Osetsky, R.E. Stoller, G.M. Stocks, 351 (2006) 109.
[10] F.v.d. Berg, W.v. Heugten, L.M. Caspers, A.v. Veen, Solid State Commun. 24 (1977) 193.
[11] H.L. Heinisch, F. Gao, R.J. Kurtz, E.A. Le, J. Nucl. Mater. 351 (2006) 141.
[12] R.J. Kurtz, H.L. Heinisch, J. Nucl. Mater. 329 (2004) 1199.
[13] M.B. Lewis, K. Farrell, Nucl. Instrum. and Meth. Phys. Res. B 16 (1986) 163.
[14] K. Ono et al., J. Nucl. Mater. 329–333 (2004) 933.
[15] T. Ishizaki, Q. Xu, T. Yoshiie, S. Nagata, Mater. Trans. 45 (2004) 9.
[16] T. Iwai, Y. Ito, M. Koshimizu, J. Nucl. Mater. 329 (2004) 963.
[17] R. Sugano, K. Morishita, A. Kimura, Fusion Sci. Technol. 44 (2003) 446.
[18] R. Vassen, H. Trinkaus, P. Jung, Phys. Rev. B 44 (1991) 4206.
[19] C.J. Ortiz, M.J. Caturla, C.C. Fu, F. Willaime, Phys. Rev. B 75 (2007) 100102.
[20] D.H. Xu, T. Bus, S.C. Glade, B.D. Wirth, J. Nucl. Mater. 367 (2007) 483.
[21] J.F. Ziegler, J.P. Biersack, U. Littmark, The Stopping and Range of Ions in Matter, Pergamon, New York, 1984.
[22] The temperature readings in Ref. [20] are not accurate, but the analysis and qualitative conclusions are not affected.
[23] D.H. Xu, B.D. Wirth, unpublished research.